

Gluon Fragmentation into Polarized Charmonium

Peter Cho¹ and Mark B. Wise²

Lauritsen Laboratory
California Institute of Technology
Pasadena, CA 91125

and

Sandip P. Trivedi³
Fermi National Accelerator Laboratory
P.O. Box 500, Batavia, IL 60510

Abstract

Gluon fragmentation to $\chi_{cJ}(1P)$ followed by single photon emission represents the dominant source of prompt J/Ψ 's at the Tevatron for $p_{\perp} \gtrsim 6$ GeV. Since fragmenting gluons are approximately transverse, their products are significantly polarized. We find that gluon fragmentation populates the helicity levels of χ_{c1} , χ_{c2} and J/Ψ according to $D_{\chi_{c1}^{(h=0)}} : D_{\chi_{c1}^{(|h|=1)}} \simeq 1 : 1$, $D_{\chi_{c2}^{(h=0)}} : D_{\chi_{c2}^{(|h|=1)}} : D_{\chi_{c2}^{(|h|=2)}} \simeq 1 : 2.9 : 6.0$ and $D_{J/\Psi^{(h=0)}} : D_{J/\Psi^{(|h|=1)}} \simeq 1 : 3.4$. We also speculate that gluon fragmentation to the radially excited $\chi_{c2}(2P)$ state followed by subsequent radiative decay could represent a large source of $\psi'(2S)$'s and potentially resolve the ψ' deficit problem. A measurement of these states' polarizations would test this idea.

8/94

¹ Work supported in part by an SSC Fellowship and by the U.S. Dept. of Energy under DOE Grant no. DE-FG03-92-ER40701.

² Work supported in part by the U.S. Dept. of Energy under DOE Grant no. DE-FG03-92-ER40701.

³ Work supported in part by DOE Contract no. DE-AC02-76CHO3000.

The production of the J/Ψ charmonium bound state is currently under active study at Fermilab [1]. Until recently, the dominant sources of J/Ψ 's at a hadron collider were believed to be parton fusion and B meson decay. These two processes respectively produce prompt and delayed J/Ψ 's which can be distinguished via B meson vertex displacement measurements. Comparison between the theoretical prediction and experimental measurement of the transverse momentum differential cross section $d\sigma(p\bar{p} \rightarrow J/\Psi + X)/dp_{\perp}$ section reveals that parton fusion alone underestimates the prompt J/Ψ production rate at high transverse momenta by approximately an order of magnitude [2,3]. Such a large discrepancy between theory and data clearly indicates that another prompt production mechanism must be at work.

Within the past few years, parton fragmentation has been examined as an alternate source of J/Ψ 's [4]. Although fragmentation takes place at higher order in perturbative QCD than quark or gluon fusion, the falloff of the former with increasing transverse momentum is much slower than that of the latter. So for $p_{\perp} \gtrsim 6$ GeV, parton fragmentation represents the dominant source of prompt J/Ψ 's.

The first charmonium fragmentation functions to be calculated were $D_{g \rightarrow J/\Psi}(z)$ and $D_{c \rightarrow J/\Psi}(z)$ which specify the probability for gluons and charm quarks to hadronize into J/Ψ as a function of its longitudinal momentum fraction z [4–6]. The only nonperturbative piece of information which enters into the lowest order computation of these S -wave fragmentation functions is the square of the charmonium bound state's wavefunction at the origin. The remainder of the calculation is based upon perturbative QCD. More recently, the fragmentation functions for gluons and charm quarks to hadronize into the lowest lying P -wave charmonium bound states χ_{c0} , χ_{c1} and χ_{c2} have been computed [7]. These χ_{cJ} states radiatively decay down to J/Ψ with the branching ratios 0.7%, 27% and 14% for $J = 0, 1$ and 2 respectively. After folding together these branching ratios with the P -wave fragmentation functions, one finds that gluon fragmentation to χ_{cJ} followed by single photon emission to J/Ψ dominates at high p_{\perp} over all other prompt mechanisms by more than an order of magnitude. When this J/Ψ source is included, the theoretical prediction for $d\sigma(p\bar{p} \rightarrow J/\Psi + X)/dp_{\perp}$ at $\sqrt{s} = 1.8$ TeV moves to within a factor of two of recent CDF data.

Most of the fragmentation functions which have been calculated to date describe the production of unpolarized quarkonium. However, it is straightforward to compute polarized fragmentation functions as well. Charm fragmentation into transverse and longitudinal J/Ψ 's was considered in refs. [6] and [8] and found to yield essentially no polarization.

J/Ψ 's produced at a lepton collider like LEP are therefore not expected to be significantly polarized. But since gluon fragmentation to χ_{cJ} represents the dominant source of J/Ψ 's at a hadron machine like the Tevatron, the polarized fragmentation functions $D_{g \rightarrow \chi_{cJ}^{(|h|)}}(z)$ where $|h| \leq J$ denotes the helicity of the produced χ_{cJ} must be determined before the degree of J/Ψ polarization can be estimated. We present the results for these fragmentation functions and the χ_{cJ} and J/Ψ polarizations which they induce in this letter.

To begin, we adopt the notation and general methods for computing P -wave fragmentation functions established in [7]. The lowest order diagrams that contribute to χ_{cJ} fragmentation are illustrated in fig. 1. They may be evaluated using standard Feynman rules for quarkonium processes [9]. The kinematic regime in which these graphs become important occurs when the lab frame energy q_0 of the incoming off-shell gluon g^* is large, but its squared four-momentum q^2 is close to the square of the charmonium bound state's mass. We therefore neglect terms which are subdominant in the ratio q^2/q_0^2 . The sum of the two diagrams in fig. 1 logarithmically diverges in the limit $z \rightarrow 1$ when the bound state carries off all the original gluon's energy and the outgoing gluon undergoes zero recoil. This infrared divergence is canceled by the diagram in fig. 2 which depicts the conversion of g^* into a color-octet 3S_1 state. The colored state can subsequently emit a soft gluon and decay to a color-singlet χ_{cJ} . The graphs in figs. 1 and 2 must be added together to obtain an infrared finite result.

To determine the polarized fragmentation functions $D_{g \rightarrow \chi_{cJ}^{(|h|)}}(z)$, we need the polarization sums for the individual helicity levels of χ_{cJ} . These spin sums may be conveniently expressed in terms of an auxiliary light-like vector $n = (1, -\hat{p})$ where \hat{p} denotes a unit vector oriented along the three-momentum of the χ_{cJ} in the lab frame. The longitudinal and transverse polarization sums for the spin-1 boson can then be simply written in the covariant forms [10]

$$\begin{aligned} \sum_{h=0} \varepsilon_{\alpha}^{(h)}(p) \varepsilon_{\beta}^{(h)}(p)^* &= P_{\alpha\beta} - P_{\alpha\beta}^T \\ \sum_{|h|=1} \varepsilon_{\alpha}^{(h)}(p) \varepsilon_{\beta}^{(h)}(p)^* &= P_{\alpha\beta}^T \end{aligned} \tag{1}$$

where

$$\begin{aligned} P_{\alpha\beta}^T &= -g_{\alpha\beta} + \frac{1}{np} (p_{\alpha} n_{\beta} + n_{\alpha} p_{\beta}) - \frac{p^2}{(np)^2} n_{\alpha} n_{\beta} \\ P_{\alpha\beta} &= -g_{\alpha\beta} + \frac{p_{\alpha} p_{\beta}}{p^2} \end{aligned} \tag{2}$$

represent two-dimensional transverse and three-dimensional projection operators. The corresponding spin-2 polarization sums are given by

$$\begin{aligned}
\sum_{h=0} \varepsilon_{\alpha\beta}^{(h)}(p) \varepsilon_{\mu\nu}^{(h)}(p)^* &= \frac{2}{3} (P_{\alpha\beta} - \frac{3}{2} P_{\alpha\beta}^T) (P_{\mu\nu} - \frac{3}{2} P_{\mu\nu}^T) \\
\sum_{|h|=1} \varepsilon_{\alpha\beta}^{(h)}(p) \varepsilon_{\mu\nu}^{(h)}(p)^* &= \frac{1}{2} \left[P_{\alpha\mu} P_{\beta\nu} + P_{\alpha\nu} P_{\beta\mu} - P_{\alpha\mu}^T P_{\beta\nu}^T - P_{\alpha\nu}^T P_{\beta\mu}^T \right] \\
&\quad + \left[P_{\alpha\beta} P_{\mu\nu}^T + P_{\alpha\beta}^T P_{\mu\nu} - P_{\alpha\beta} P_{\mu\nu} - P_{\alpha\beta}^T P_{\mu\nu}^T \right] \\
\sum_{|h|=2} \varepsilon_{\alpha\beta}^{(h)}(p) \varepsilon_{\mu\nu}^{(h)}(p)^* &= \frac{1}{2} \left[P_{\alpha\mu}^T P_{\beta\nu}^T + P_{\alpha\nu}^T P_{\beta\mu}^T - P_{\alpha\beta}^T P_{\mu\nu}^T \right].
\end{aligned} \tag{3}$$

After a straightforward computation,¹ we obtain the polarized χ_{cJ} fragmentation functions:

$$\begin{aligned}
D_{g \rightarrow \chi_{c0}}(z, M) &= \frac{4}{81} \frac{H_1 \alpha_s(M)^2}{M} \left[\frac{1}{(1-z)_+} + \left(\frac{13}{12} - \log \frac{2\Lambda}{M} \right) \delta(1-z) - 1 + \frac{85}{8} z - \frac{13}{4} z^2 \right. \\
&\quad \left. + \frac{9}{4} (5-3z) \log(1-z) \right] + \frac{1}{12} \frac{\pi \alpha_s(M) H_8'(\Lambda)}{M} \delta(1-z)
\end{aligned} \tag{4}$$

$$\begin{aligned}
D_{g \rightarrow \chi_{c1}^{(h=0)}}(z, M) &= \frac{4}{81} \frac{H_1 \alpha_s(M)^2}{M} \left[\frac{3}{2(1-z)_+} + \left(\frac{13}{8} - \frac{3}{2} \log \frac{2\Lambda}{M} \right) \delta(1-z) - \frac{3}{2} - \frac{3}{4} z - \frac{3}{2} z^2 \right] \\
&\quad + \frac{1}{8} \frac{\pi \alpha_s(M) H_8'(\Lambda)}{M} \delta(1-z)
\end{aligned} \tag{5a}$$

$$\begin{aligned}
D_{g \rightarrow \chi_{c1}^{(|h|=1)}}(z, M) &= \frac{4}{81} \frac{H_1 \alpha_s(M)^2}{M} \left[\frac{3}{2(1-z)_+} + \left(\frac{5}{4} - \frac{3}{2} \log \frac{2\Lambda}{M} \right) \delta(1-z) - \frac{3}{2} - \frac{3}{2} z^2 \right] \\
&\quad + \frac{1}{8} \frac{\pi \alpha_s(M) H_8'(\Lambda)}{M} \delta(1-z)
\end{aligned} \tag{5b}$$

$$\begin{aligned}
D_{g \rightarrow \chi_{c2}^{(h=0)}}(z, M) &= \frac{4}{81} \frac{H_1 \alpha_s(M)^2}{M} \left[\frac{1}{2(1-z)_+} + \left(\frac{13}{24} - \frac{1}{2} \log \frac{2\Lambda}{M} \right) \delta(1-z) \right. \\
&\quad + 108z^{-3} - 216z^{-2} + 117z^{-1} - \frac{19}{2} - \frac{5}{4} z - \frac{1}{2} z^2 \\
&\quad \left. + 54 \frac{(2-z)(1-z)^2}{z^4} \log(1-z) \right] + \frac{1}{24} \frac{\pi \alpha_s(M) H_8'(\Lambda)}{M} \delta(1-z)
\end{aligned} \tag{6a}$$

¹ We used the high energy physics Mathematica package FeynCalc to perform much of the tedious algebra [11].

$$\begin{aligned}
D_{g \rightarrow \chi_{c2}^{(|h|=1)}}(z, M) &= \frac{4}{81} \frac{H_1 \alpha_s(M)^2}{M} \left[\frac{3}{2(1-z)_+} + \left(\frac{5}{4} - \frac{3}{2} \log \frac{2\Lambda}{M} \right) \delta(1-z) \right. \\
&\quad - 144z^{-3} + 288z^{-2} - 228z^{-1} + \frac{165}{2} - 6z - \frac{3}{2}z^2 \\
&\quad \left. - 36 \frac{(2-z)(1-z)}{z^4} (z^2 - 2z + 2) \log(1-z) \right] + \frac{1}{8} \frac{\pi \alpha_s(M) H_8'(\Lambda)}{M} \delta(1-z)
\end{aligned} \tag{6b}$$

$$\begin{aligned}
D_{g \rightarrow \chi_{c2}^{(|h|=2)}}(z, M) &= \frac{4}{81} \frac{H_1 \alpha_s(M)^2}{M} \left[\frac{3}{(1-z)_+} + \left(\frac{13}{4} - 3 \log \frac{2\Lambda}{M} \right) \delta(1-z) \right. \\
&\quad + 36z^{-3} - 72z^{-2} + 111z^{-1} - 78 + 21z - 3z^2 \\
&\quad \left. + 9 \frac{(2-z)}{z^4} (z^4 - 4z^3 + 6z^2 - 4z + 2) \log(1-z) \right] + \frac{1}{4} \frac{\pi \alpha_s(M) H_8'(\Lambda)}{M} \delta(1-z).
\end{aligned} \tag{6c}$$

In these expressions, $M \simeq 2m_c$ denotes the charmonium bound state's mass, Λ represents the infrared cutoff, and $H_1 = 72|R_1'(0)|^2/(\pi M^4)$ and $H_8'(\Lambda) = 8|R_0^{(8)}(0)|^2/(3\pi M^2)$ respectively contain the squares of the derivative of the color-singlet P -wave and color-octet S -wave radial wavefunctions. If the polarized fragmentation functions are summed over their helicity levels, we recover the unpolarized P -wave fragmentation functions reported in ref. [7].²

We adopt the parameter values $M = 3500$ MeV and $\alpha_s(M) = 0.24$. Following [7], we also set the infrared cutoff to $\Lambda = M/2$ and take $H_1 \simeq 15$ MeV and $H_8'(M/2) \simeq 3$ MeV. The functions in eqns. (4) - (6) can be evolved from the charmonium scale to higher energies using the Altarelli-Parisi equation and folded together with the gluon cross section $d\sigma(p\bar{p} \rightarrow g + X)/dp_\perp$ to obtain the transverse momentum distribution of χ_{cJ} 's produced at the Tevatron:

$$\frac{d\sigma(p\bar{p} \rightarrow \chi_{cJ}^{(|h|)} + X)}{dp_\perp} = \int_0^1 dz \frac{d\sigma(p\bar{p} \rightarrow g(p_\perp/z) + X, \mu)}{dp_\perp} D_{g \rightarrow \chi_{cJ}^{(|h|)}}(z, \mu). \tag{7}$$

Since the gluon cross section is a very rapidly decreasing function of p_\perp , it is a good approximation to evaluate the integral in (7) retaining just the terms proportional to

² The longitudinal and transverse χ_{c1} fragmentation functions were calculated in ref. [12]. Our results in eqns. (5a) and (5b) agree with those in [12] for $z \neq 1$ but differ for $z = 1$.

$\delta(1 - z)$ in the fragmentation functions: ³

$$\begin{aligned}
D_{g \rightarrow \chi_{c0}}(z, M) &\simeq 0.66 \times 10^{-4} \delta(1 - z) + \dots \\
D_{g \rightarrow \chi_{c1}^{(h=0)}}(z, M) &\simeq 1.00 \times 10^{-4} \delta(1 - z) + \dots \\
D_{g \rightarrow \chi_{c1}^{(|h|=1)}}(z, M) &\simeq 0.95 \times 10^{-4} \delta(1 - z) + \dots \\
D_{g \rightarrow \chi_{c2}^{(h=0)}}(z, M) &\simeq 0.33 \times 10^{-4} \delta(1 - z) + \dots \\
D_{g \rightarrow \chi_{c2}^{(|h|=1)}}(z, M) &\simeq 0.95 \times 10^{-4} \delta(1 - z) + \dots \\
D_{g \rightarrow \chi_{c2}^{(|h|=2)}}(z, M) &\simeq 1.99 \times 10^{-4} \delta(1 - z) + \dots
\end{aligned} \tag{8}$$

Longitudinally and transversely polarized χ_{c1} 's are therefore produced at the Tevatron in the ratio $D_{\chi_{c1}^{(h=0)}} : D_{\chi_{c1}^{(|h|=1)}} \simeq 1 : 1$, while the helicity levels of χ_{c2} are populated according to $D_{\chi_{c2}^{(h=0)}} : D_{\chi_{c2}^{(|h|=1)}} : D_{\chi_{c2}^{(|h|=2)}} \simeq 1 : 2.9 : 6.0$. Comparing these $J = 1$ and $J = 2$ ratios to their unpolarized counterparts $D_{\chi_{c1}^{(h=0)}} : D_{\chi_{c1}^{(|h|=1)}} = 1 : 2$ and $D_{\chi_{c2}^{(h=0)}} : D_{\chi_{c2}^{(|h|=1)}} : D_{\chi_{c2}^{(|h|=2)}} = 1 : 2 : 2$, we clearly see that the χ_{c1} and χ_{c2} states produced as a result of gluon fragmentation are significantly polarized.

The source of this sizable χ_{cJ} polarization can be traced to the fragmenting gluon. If the gluon were on-shell, its polarization would be completely transverse. The extent to which g^* is actually off-shell modifies this result by only $O(q^2/q_0^2)$ terms. This effect can be seen most simply in the diagram of fig. 2. The color-octet 3S_1 $c\bar{c}$ in the $|\bar{c}\bar{c}g\rangle$ Fock state must inherit the gluon's polarization in order to conserve angular momentum. The subsequent transformation of this state into χ_{c1} and χ_{c2} populates their respective $|h| = 0, 1$ and $|h| = 0, 1, 2$ helicity levels in the ratios 1:1 and 1:3:6. As the color-octet terms in eqns. (4) - (6) numerically dominate over the color-singlet terms, this explanation accounts in large part for the χ_{cJ} polarization which we have found.

We now turn to consider the radiative decay $\chi_{cJ} \rightarrow J/\Psi + \gamma$. Since the electromagnetic branching ratio for χ_{c0} is more than an order of magnitude smaller than those for χ_{c1} and χ_{c2} , we neglect its contribution to J/Ψ production. The invariant amplitudes for the remaining $J^{PC} = (1, 2)^{++}$ P -wave charmonium states to decay via E1 transitions to the $J^{PC} = (1)^{--}$ S -wave state must be parity even, charge conjugation symmetric and electromagnetic gauge invariant. They can be written down by inspection:

$$\begin{aligned}
i\mathcal{A}(\chi_{c1}(p) \rightarrow J/\Psi(p - k) + \gamma(k)) &= g_1 \epsilon^{\mu\nu\alpha\beta} k_\mu \epsilon_\nu^{(\chi_{c1})} \epsilon_\alpha^{(J/\Psi)} \epsilon_\beta^{(\gamma)} \\
i\mathcal{A}(\chi_{c2}(p) \rightarrow J/\Psi(p - k) + \gamma(k)) &= g_2 p^\mu \epsilon_{(\chi_{c2})}^{\alpha\beta} \epsilon_\alpha^{(J/\Psi)} [k_\mu \epsilon_\beta^{(\gamma)} - k_\beta \epsilon_\mu^{(\gamma)}].
\end{aligned} \tag{9}$$

³ Altarelli-Parisi evolution approximately cancels in the ratios of fragmentation functions. We therefore neglect it in our polarization analysis.

Given these amplitudes, we can determine the photon's angular distribution in the χ_{cJ} rest frame. Letting θ denote the angle between the photon's three-momentum in this frame and the χ_{cJ} 's three-momentum in the lab frame, we form the dimensionless ratio

$$R^{(J)}(\cos \theta) = \sum_{h=-J}^J \frac{D_{g \rightarrow \chi_{cJ}^{(h)}}}{D_{g \rightarrow \chi_{cJ}}} \frac{\frac{d\Gamma}{d\cos \theta}(\chi_{cJ}^{(h)} \rightarrow J/\Psi + \gamma)}{\Gamma(\chi_{cJ} \rightarrow J/\Psi + \gamma)} \quad (10)$$

which is a convenient measure of the angular distribution of photons from polarized χ_{cJ} 's. The explicit dependence of $R^{(J)}$ upon $\cos \theta$ is given by

$$\begin{aligned} R^{(1)}(\cos \theta) &= \frac{3}{8} \left[\left(1 + \frac{\rho}{2}\right) + \left(1 - \frac{3}{2}\rho\right) \cos^2 \theta \right] \\ R^{(2)}(\cos \theta) &= \frac{3}{4} \left[\left(\frac{5}{6} - \frac{\sigma}{12} - \frac{\tau}{3}\right) - \left(\frac{1}{2} - \frac{\sigma}{4} - \tau\right) \cos^2 \theta \right] \end{aligned} \quad (11)$$

where $\rho = D_{g \rightarrow \chi_{c1}^{(|h|=1)}}/D_{g \rightarrow \chi_{c1}}$, $\sigma = D_{g \rightarrow \chi_{c2}^{(|h|=1)}}/D_{g \rightarrow \chi_{c2}}$ and $\tau = D_{g \rightarrow \chi_{c2}^{(|h|=2)}}/D_{g \rightarrow \chi_{c2}}$. If χ_{c1} and χ_{c2} were unpolarized, then $\rho = 2/3$, $\sigma = \tau = 2/5$ and $R^{(J)}$ would become independent of $\cos \theta$. But the fragmentation results in eqn. (8) imply $\rho \simeq 0.49$, $\sigma \simeq 0.29$ and $\tau \simeq 0.61$ and yield

$$R^{(1)}(\cos \theta) \simeq 0.47 [1 + 0.21 \cos^2 \theta] \quad (12a)$$

$$R^{(2)}(\cos \theta) \simeq 0.46 [1 + 0.30 \cos^2 \theta]. \quad (12b)$$

In principle, measurements of $R^{(1)}$ and $R^{(2)}$ would determine the polarizations of χ_{c1} and χ_{c2} . But in practice, it will be much easier to observe the average angular distribution

$$R^{(\text{avg})}(\cos \theta) = \frac{\sum_{J=1}^2 D_{g \rightarrow \chi_{cJ}} \text{Br}(\chi_{cJ} \rightarrow J/\Psi + \gamma) R^{(J)}(\cos \theta)}{\sum_{J=1}^2 D_{g \rightarrow \chi_{cJ}} \text{Br}(\chi_{cJ} \rightarrow J/\Psi + \gamma)} \simeq 0.47 [1 + 0.25 \cos^2 \theta] \quad (13)$$

and extract an average χ_{cJ} polarization.

The amplitude expressions in (9) can also be used to derive the polarization of the J/Ψ which is induced by its χ_{cJ} progenitor. The feeddown from the separate χ_{cJ} helicity modes to those of the J/Ψ is given by

$$\begin{aligned} D_{J/\Psi^{(h=0)}} &= \text{Br}(\chi_{c1} \rightarrow J/\Psi + \gamma) \left[\frac{1}{2} D_{\chi_{c1}^{(|h|=1)}} \right] + \text{Br}(\chi_{c2} \rightarrow J/\Psi + \gamma) \left[\frac{2}{3} D_{\chi_{c2}^{(h=0)}} + \frac{1}{2} D_{\chi_{c2}^{(|h|=1)}} \right] \\ D_{J/\Psi^{(|h|=1)}} &= \text{Br}(\chi_{c1} \rightarrow J/\Psi + \gamma) \left[D_{\chi_{c1}^{(h=0)}} + \frac{1}{2} D_{\chi_{c1}^{(|h|=1)}} \right] \\ &\quad + \text{Br}(\chi_{c2} \rightarrow J/\Psi + \gamma) \left[\frac{1}{3} D_{\chi_{c2}^{(h=0)}} + \frac{1}{2} D_{\chi_{c2}^{(|h|=1)}} + D_{\chi_{c2}^{(|h|=2)}} \right]. \end{aligned} \quad (14)$$

After inserting the radiative branching ratios and χ_{cJ} fragmentation probabilities, we find that longitudinal and transverse J/Ψ 's are produced in the ratio $D_{J/\Psi(h=0)} : D_{J/\Psi(|h|=1)} \simeq 1 : 3.4$. Equivalently, the ratio of transversely polarized to total J/Ψ 's equals $\zeta \simeq 0.77$. This ratio may be measured in the leptonic decay $J/\Psi \rightarrow \ell^+\ell^-$. If Θ represents the angle between the lepton three-momentum in the J/Ψ rest frame and the three-momentum of the J/Ψ in the lab frame, then

$$\frac{d\Gamma}{d\cos\Theta}(\psi \rightarrow \ell^+\ell^-) = \frac{3}{4} \left[\left(1 - \frac{\zeta}{2}\right) - \left(1 - \frac{3}{2}\zeta\right) \cos^2\Theta \right] \simeq 0.46 [1 + 0.25 \cos^2\Theta]. \quad (15)$$

J/Ψ production via gluon fragmentation to χ_{cJ} consequently induces a 25% shift in the lepton pair angular distribution relative to unpolarized J/Ψ 's.

The χ_{cJ} and J/Ψ polarizations that we have found represent model independent predictions of QCD which can be experimentally tested. Verification of these results would provide nontrivial checks of the entire fragmentation picture of quarkonium production at large p_\perp .

We have so far considered the production of only the lowest lying $n = 1$ radial level charmonium states. However, fragmentation ideas can be simply applied to higher radial levels as well. In particular, gluon and charm fragmentation to $\psi'(2S)$ have been studied in ref. [2]. Even when fragmentation is included along with direct production, the theoretical prediction for ψ' production underestimates the number of ψ' 's which have been observed at the Tevatron by roughly a factor of 50. This large gap between theory and data strongly suggests that some important ψ' production mechanism still remains to be included.

It is important to recall that ψ' is the heaviest $c\bar{c}$ bound state which lies below the $D\bar{D}$ threshold. Therefore, $n = 1$ χ_{cJ} states cannot radiatively decay to ψ' , but their $n = 2$ counterparts can. None of these latter states which lie above the $D\bar{D}$ threshold have been observed. Estimates for their masses yield $M(\chi_{c0}(2P)) = 3920$ MeV, $M(\chi_{c1}(2P)) = 3950$ MeV and $M(\chi_{c2}(2P)) = 3980$ MeV [13]. These mass values kinematically allow the S -wave transitions $\chi_{c0}(2P) \rightarrow D\bar{D}$ and $\chi_{c1}(2P) \rightarrow D^*\bar{D}$ to occur. We therefore expect the $J = 0$ and $J = 1$ excited χ_{cJ} 's to be broad and to have negligible branching fractions to lower $c\bar{c}$ bound states. However, angular momentum and parity considerations require the analogous decays $\chi_{c2}(2P) \rightarrow D\bar{D}$ and $\chi_{c2}(2P) \rightarrow D^*\bar{D}$ for the $J = 2$ state to proceed via $L = 2$ partial waves. Although we cannot readily compute by how much these D -wave decays will be suppressed, it is possible that the branching fractions for $\chi_{c2}(2P)$ transitions

to charmonium states below $D\bar{D}$ threshold could be significant.⁴ If so, the experimentally measured branching fraction $\text{Br}(\chi_{b2}(2P) \rightarrow \Upsilon(2S) + \gamma) = 19\%$ in the $b\bar{b}$ sector suggests that the corresponding fraction $\text{Br}(\chi_{c2}(2P) \rightarrow \psi'(2S) + \gamma)$ could lie in the few percent range. We estimate that a 5% branching fraction would enhance the theoretical prediction for ψ' production by more than an order of magnitude. Such an enhancement would help resolve the ψ' deficit problem.

Our proposal is admittedly speculative. If this idea is correct, then a ψ' should be accompanied by a photon resulting from $\chi_{c2}(2P)$ decay. Since the $\chi_{c2}(2P)$ is polarized to approximately the same extent as its $n = 1$ counterpart, the photon will be distributed in angle according to $R^{(2)}(\cos \theta)$ as specified in eqn. (12b). Moreover, the induced polarization for ψ' should be slightly enhanced relative to that of J/Ψ since $\chi_{c1}(2P)$ does not feed down along with $\chi_{c2}(2P)$. A measurement of these radially excited states' polarizations would therefore provide a test of this possible ψ' production mechanism.

⁴ The 1D_2 charmonium state is forbidden from decaying to $D\bar{D}$ by parity. Moreover, its mass is predicted to lie below the $D^*\bar{D}$ threshold [13]. This state is therefore narrow. However, its production is suppressed, and it is expected to have a very small branching ratio to $\psi'\gamma$. The contribution of the 1D_2 state to ψ' production is consequently negligible.

References

- [1] CDF Collaboration, Fermilab-conf-94/136-E (1994), unpublished.
- [2] E. Braaten, M. A. Doncheski, S. Fleming and M. L. Mangano, Fermilab-pub-94/135-T (1994), unpublished.
- [3] M. Cacciari and M. Greco, FNT/T-94/13 (1994), unpublished.
- [4] E. Braaten and T.C. Yuan, Phys. Rev. Lett. **71** (1993) 1673.
- [5] E. Braaten, K. Cheung and T.C. Yuan, Phys. Rev. **D48** (1993) 4230.
- [6] Y.-Q. Chen, Phys. Rev. **D48** (1993) 5181.
- [7] E. Braaten and T.C. Yuan, Fermilab-pub-94/040-T (1994), unpublished.
- [8] A. Falk, M. Luke, M. Savage and M. Wise, Phys. Lett **B312** (1993) 486.
- [9] J. H. Kühn, J. Kaplan and E. G. O. Safiani, Nucl. Phys. **B157** (1979) 125;
B. Guberina, J.H. Kühn, R.D. Peccei and R. Rückl, Nucl. Phys. **B174** (1980) 317.
- [10] K. Cheung and T. C. Yuan, NUHEP-TH-94-7 (1994), unpublished.
- [11] R. Mertig, M. Böhm and A. Denner, Comp. Phys. Comm. **64** (1991) 345.
- [12] J. P. Ma, Phys. Lett. **B332** (1994) 398.
- [13] S. Godfrey and N. Isgur, Phys. Rev. **D32** (1985) 189.

Figure Captions

- Fig. 1. Lowest order Feynman diagrams which mediate gluon fragmentation to color-singlet P-wave charmonium bound states.
- Fig. 2. Lowest order Feynman diagram which mediates gluon fragmentation to a color-octet S-wave charmonium state.

This figure "fig1-1.png" is available in "png" format from:

<http://arXiv.org/ps/hep-ph/9408352v1>

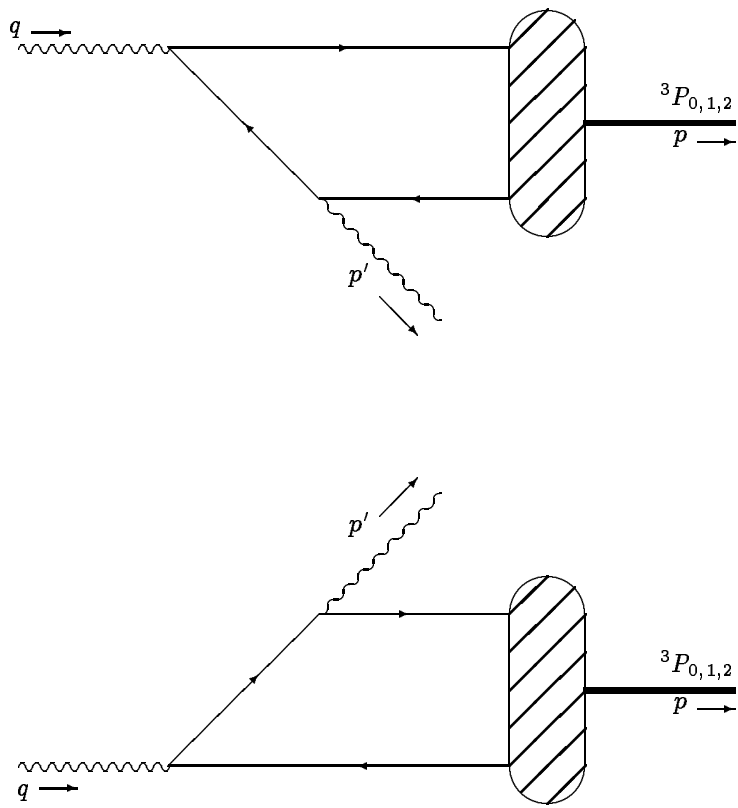


Figure 1

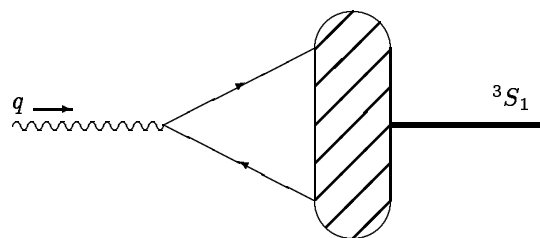


Figure 2